

PRVPATENT- OCH REGISTRERINGSVERKET
Patentavdelningen

REC'D 28 FEB 2005

WIPO

PCT

**Intyg
Certificate**

Härmed intygas att bifogade kopior överensstämmer med de handlingar som ursprungligen ingivits till Patent- och registreringsverket i nedannämnda ansökan.

This is to certify that the annexed is a true copy of the documents as originally filed with the Patent- and Registration Office in connection with the following patent application.



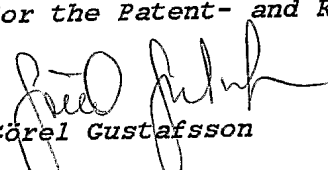
(71) Sökande Anders Johansson, Norrköping SE
Applicant (s) Tommy Sundqvist, Linköping SE
Åke Öberg, Ljungsbro SE

(21) Patentansökningsnummer 0400145-9
Patent application number

(86) Ingivningsdatum 2004-01-27
Date of filing

Stockholm, 2005-02-04

För Patent- och registreringsverket
For the Patent- and Registration Office


Görel Gustafsson

Avgift
Fee

**PRIORITY
DOCUMENT**

SUBMITTED OR TRANSMITTED IN
COMPLIANCE WITH RULE 17.1(a) OR (b)

**PATENT- OCH
REGISTRERINGSVERKET
SWEDEN**

Postadress/Address
Box 5055
S-102 42 STOCKHOLM

Telefon/Phone
+46 8 782 25 00
Vx 08-782 25 00

Telex
17978
PATOREG S

Telefax
+46 8 666 02 86
08-666 02 86

AN ARRANGEMENT AND METHOD FOR ASSESSING JOINTS

Technical Field

The present invention generally relates to an arrangement and a measurement method
5 for assessing joints. More specifically, the present invention relates to an arrangement
and a method for measuring joint cartilage quality, such as cartilage thickness, cartilage
surface roughness and degree of cartilage fibrillation. The arrangement comprises an
arthroscopic probe and means for light source driving/control, light detection, signal
processing and presentation.

10

Prior art

Arthritis is a group of common, chronic diseases with great consequences for the
individual patient and society. The prevalence of osteoarthritis, for instance, increases
after 50 years of age, with women at greater risk than men. Factors that increase the risk
15 of arthritis are sport and work related injuries and overweight (PEYRON, 1986).

Arthroscopy has been used for the diagnosis and therapy of orthopedic disorders since
the beginning of the twentieth century. Takagi (TAGAKI, 1918, in ALTMAN and
KATES, 1983) modified a pediatric cytoscope to fit the problem area of knee joint
visualization which became the birth of this dynamic and rewarding field. The
20 arthroscope is primarily a diagnostic device but therapeutic variants allow the removal
of adhesions, intra-articular debris and meniscectomy (JACKSON, 1983). The
arthroscope gives visual information from the interior of a joint, transmitted via optical
fibres to the human eye. Demands have been raised, though, that a more quantitative
approach in diagnostic work would improve the quality of therapeutic decisions.

25 Thickness of cartilage, cartilage surface roughness and the degree of cartilage fibrillation
are all parameters of great interest in a more quantitative approach to cartilage
diagnostics.

Many researchers have earlier suggested ways for cartilage thickness assessment.
Several of the methods suggested require a disarticulation of the joint. Usually, these
30 methods measure the undeformed thickness of the cartilage layer. Armstrong and Mow
(ARMSTRONG and MOW, 1982) developed an optical method, applied to an isolated
cartilage/bone specimen, in which the cartilage/bone interface was easily detected.
Needle probe methods (HOCH et al., 1983; MOW et al., 1989; RÄSÄNEN et al., 1990)
measure force and displacement of a sharp needle penetrating the cartilage layer from

which cartilage thickness can be calculated. The needle method does not require an isolated specimen, and *in situ* surfaces can be tested. Jurvelin (JURVELIN et al., 1995) has compared microscopy based measurements, the needle probe method and the ultrasound technique. The linear correlation coefficient between microscopy and the
5 needle probe measurements was 0.97 ($n = 80$) and 0.91 ($n = 45$) between microscopy and ultrasonic measurements. Strong correlation was also obtained between the needle probe measurements and the ultrasonic measurements. The difference between the three methods is of the order of 0.1 mm or less at a mean sample thickness of 0.86 mm. The authors conclude that the three different techniques for cartilage thickness measurements
10 are highly related.

In situ cartilage thickness has also been measured with high resolution ultrasound (MODEST et al., 1989; RUSHFELDT et al., 1981). Wayne (WAYNE et al., 1998) utilized a radiographic and image analyzing method for thickness studies in articulated joints. Swann and Seedhom (SWANN and SEEDHOM, 1989) described an improved
15 needle technique for thickness measurements. These authors all question the methods which disrupt the cartilage layer because of the thickness changes caused by dehydration or hydrophilic swelling. However, the authors report an accuracy of ± 0.012 mm with a repeatability of 1.2% for the needle probe.

Optical coherence tomography (OCT) has recently been suggested as a tool to assess
20 articular cartilage structure and thickness (HERRMANN et al., 1999; DREXLER et al., 2000). OCT is based on interferometry between light from a scanning mirror and the cartilage sample. Hermann et al. report resolutions of 5 – 15 μm and differences between OCT and histological measurements of the order of 7 – 9 %. Drexler et al. suggest that polarisation sensitive OCT (PSOCT) can be advantageous for the
25 quantification of collagen structure changes, associated with osteoarthritis.

Magnetic resonance imaging (MRI) has been increasingly used to assess articular cartilage injuries and arthritis. *In vitro* bovine knees have been examined with MRI (MAH et al., 1990). Signal variations have been noticed in degenerated cartilage (LEHNER et al., 1989). MRI has also been used *in vivo* in a canine arthritis model
30 (BRAUNSTEIN et al., 1990). These studies showed hypertrophic articular cartilage repair and other changes associated with osteoarthritis. MRI has also been used increasingly in human studies (for a review see RECHT and RESNICK, 1994). Many of the studies in humans are knee studies with a focus on the identification of focal defects

and cartilage thickness. In these studies the arthroscopy method is often referred to as the gold standard.

Roentgenological techniques have also been used for cartilage studies. Double-contrast techniques (HALL and WYSHAK, 1980) have been frequently used in thickness studies in relation to sex, weight and height.

Reflection spectroscopy is a well-established method for investigation of the structural/molecular composition of a tissue volume. Light from a broad band light source is brought to impinge on the tissue. The light is absorbed and scattered in the tissue volume. The detected spectral distribution of diffusely scattered light carries information about the molecular/structural composition of the tissue passed by the photons.

Cartilage behaves spectroscopically almost like a sheet of white paper whereas the underlying bone has a very different reflection spectrum. The differences can partly be explained by the haemoglobin content of bone. Bone is perfused with blood as opposed to cartilage which is nutritionally supported from the joint liquor.

The source of inspiration to the present work is the clinically expressed demand to perform cartilage thickness measurements during arthroscopic assessments of joints. A spectroscopic method for this purpose would be easily combined with, or integrated into, an arthroscope that would permit simultaneous conventional arthroscopic investigations with quantitative measurements of cartilage thickness. In a longer perspective, it is probably possible to utilize optical fibre measurements for a variety of other important properties such as bone perfusion, cartilage surface topology and degree of fibrillation (NÖTZLI et al., 1989; HANDLEY et al., 1990; DREXLER et al., 2000).

Summary of the invention

The invention is based on the differences in the optical properties of cartilage and subchondral bone. Bone is perfused with blood whereas cartilage mainly consists of collagen fibers and proteoglycan aggregates. The two substances thus show marked differences in absorption spectrum and scattering. The described arthroscope provides joint surface illumination and back-scattered light is analyzed by a signal processor. According to described procedures, thinner sections of cartilage is found by studying intensity quotas for selected wavelengths, and arthritic/diseased cartilage is seen by studying changes in polarisation of the initial light. Two approaches are presented, one describing a single point measurement and one describing an imaging technique.

Description of the Drawings

Fig. 1 is the Monte Carlo model used for simulations including a cartilage layer of known thickness on top of a semi-infinite bone layer containing blood. The number of photons (out of incident 10^6) back-scattered to a ring shaped detector is calculated.

Fig. 2 upper graph shows mean reflection spectra from the reference material, including cartilage (dark line, $n = 23$) and bone containing blood (bright line, $n = 10$). Whiskers show \pm SD. Lower graph shows reference spectrum of blood (TAKATANI and GRAHAM, 1979).

Fig. 3 shows examples of reflectance spectra from a grinding session. Before grinding ($d = 1.66$ mm), after first grinding ($d = 0.78$ mm), after third grinding ($d = 0.44$ mm) and after fourth grinding ($d = 0$ mm). Reference spectra of cartilage and bone containing blood are included for comparison. The spectra are separated in the y-direction for clarity.

Fig. 4 shows spectroscopically estimated cartilage thickness measure (d_{spec}) plotted against reference cartilage thickness for the complete material.

Fig. 5 shows Monte Carlo simulation results, including detected photons out of 10^6 ejected (in per cent) for increasing cartilage layer thicknesses. The simulations are performed for the single wavelength 633 nm.

25

Fig. 6 is a schematic drawing of a suggested arthroscopic probe and

Fig. 7 is a schematic drawing of the suggested arrangement.

30

Detailed description

Materials and methods

- Twelve hip joint condyles from bovine calves were obtained from a local slaughterhouse less than 24 hours after sacrifice. Two of the condyles were used for reference measurements and the other ten for thickness experiments. The condyles were stored in saline in a refrigerator and prepared for cartilage measurements through the removal of soft tissues and tendons surrounding the joint.
- Three sites on each condyle surface were used for the measurements. A handheld, rotating, grinding machine was used to reduce the cartilage layer thickness. Sandpaper with the roughness P100 was used for grinding. Care was taken to grind in short episodes (5 – 15 s) so as not to increase the temperature of the cartilage. Thickness measurement of the cartilage layer was done with a high-resolution ultrasound scanner (B-mode 20MHz, Dermascan 3v3, Cortex Technology, Hadsund, Denmark). The probe scanned over the measurement site and an image of the cartilage/bone interface was presented on the computer screen.
- Optical reflection spectra were recorded by using an Oriel Instaspec IV CCD spectrometer equipped with an Ocean Optics broad spectrum tungsten lamp HL 2000 (spectral range 360 – 2000 nm). The light was guided by optical glass fibre bundles (NA = 0.35) and the measurements were taken at a small distance (2 – 5mm) to the condyle surface. The bundles were arranged in a probe head (diameter 4 mm) with the emitting fibre bundle encircling the detecting bundle. The reflection spectra were calculated according to the formula:

$$I(\lambda) = \frac{I_{tissue} - I_{background}}{I_{reference} - I_{background}} \quad (1)$$

where I_{tissue} is the raw spectrum of the examined tissue, $I_{background}$ the detector background signal, and $I_{reference}$ the diffuse reflectance spectrum taken from a white reference ($BaSO_4$).

For each measurement position, spectra and ultrasound images were recorded from the intact cartilage layer, for 4 - 5 intermediate cartilage thicknesses (obtained by grinding) and when bone level had been reached.

- 5 Twenty-three pieces of pure cartilage, about 1 mm thick, were removed from the two joints by using a sharp knife. Remains of subchondral bone were carefully removed to secure a pure cartilage sample. Reflection spectra were measured, with the equipment described above, for each piece of cartilage placed on a black plastic sheet. The joints were cut in half, washed in saline and stored (in saline) for a few days to remove
10 remains of blood. Finally, reflection spectra were taken from 10 positions on the exposed bone samples. Mean reference spectra for cartilage ($n = 23$) and bone ($n = 10$) were calculated and will be referred to as $S_{cartilage}$ and S_{bone} , respectively. Furthermore, the reference spectrum of blood (S_{blood}) was estimated as the inverse absorption spectrum of oxyhaemoglobin, taken from the literature (TAKATANI and GRAHAM,
15 1979). To decrease the influence of remains of blood in the bone, S_{bone} was adjusted by subtracting S_{blood} until the characteristic haemoglobin peaks could no longer be distinguished.

- Each measured reflectance spectrum was matched to the true cartilage thickness (d), as
20 determined from the stored ultrasound images. For the thickness determination, the manufacturer's software including a cursor system was used. The resolution of the ultrasound image was 0.06 mm. As a measure of cartilage thickness, determined from the spectroscopic data, d_{spec} was defined as the percentage contribution (%) of cartilage spectrum in the measured reflectance spectrum:

25

$$d_{spec} = \frac{a}{a + b + c} \quad (2)$$

where a , b and c are the coefficients for optimal match (least square fitting) between the measured spectrum ($S_{measured}$) and the reference spectra according to:

30

$$S_{measured} = a \cdot S_{cartilage} + b \cdot S_{bone} + c \cdot S_{blood} \quad (3)$$

An exponential regression model (4) was used for statistical comparison between reference cartilage thickness and d_{spec} .

$$d_{spec} = K_1(1 - e^{-K_2 \cdot d}) \quad (4)$$

5

where K_1 and K_2 are constants.

In order to test the assumption of an exponential relation between the cartilage thickness d and the corresponding spectroscopic data, a Monte Carlo model was used (Fig. 1). The model has a cartilage layer of known thickness (d) and diffusion theory optical properties (μ_{ac} , μ_{sc} , g_c) positioned on top of a semi-infinite layer of bone containing blood (μ_{ab} , μ_{sb} , g_b). The optical properties of cartilage, bone and blood were taken from the literature (BEEK et al., 1997; FIRBANK et al., 1993; TUCHIN, 2000) for the single wavelength 633 nm (see discussion). The optical properties of bone containing blood were set to the bone coefficients increased by those of blood at a selected perfusion level (10%) according to:

$$\mu_{ab} = \mu_{a,bone} + 0.10 \cdot \mu_{a,blood} \quad (5.1)$$

$$\mu_{sb} = \mu_{s,bone} + 0.10 \cdot \mu_{s,blood} \quad (5.2)$$

$$g_b = g_{bone} + 0.10 \cdot (g_{blood} - g_{bone}) \quad (5.3)$$

20

All optical parameters are presented in Table 1. Refractive indices of both layers were set to 1 as specular effects were not of interest. The pathways of 10^6 photons, incident in a point at the cartilage surface, were calculated (DE MUL et al., 1995). The back-scattered photons reaching a ring shaped detector (outer radius 3 mm, inner radius 1 mm) were counted. Simulations were performed for cartilage thicknesses $d = 0 - 3$ mm in steps of 0.1 mm.

25

Table 1 Tissue optical properties used in the Monte Carlo simulations

	Absorption coefficient μ_a [mm ⁻¹]	Scattering coefficient μ_s [mm ⁻¹]	Anisotropy factor g
Cartilage	0.033	21.4	0.909
Bone	0.040	35.0	0.925
Blood	1.60	413	0.997
Bone containing blood	0.20	76.3	0.932

5 Results

The mean reflection spectra of the reference material are presented in Fig. 2. The cartilage spectrum appears relatively “white” with a shift towards the blue region, whilst the bone spectrum appears distinctly “red” and includes the characteristic absorption peaks of haemoglobin at 542 nm and 576 nm. In the thickness analysis, the latter spectrum is divided into S_{bone} and S_{blood} (see Equation 3).

The mean (\pm SD) thickness of intact cartilage was 1.21 ± 0.30 mm ($n = 30$). A typical example of spectra from a grinding sequence is shown in Fig. 3. As the cartilage layer gets thinner a clear influence of bone can be seen. The spectroscopic estimation of cartilage thickness (d_{spec}) is plotted against the ultrasound reference cartilage thickness in Fig. 4. The regression model of Equation 4 is used ($r = 0.69$, $p < 0.000001$, $s = 0.167$, $K_1 = 0.75$, $K_2 = 3.81$, $n = 182$). For thinner cartilage layers ($d < 0.5$ mm), the model mean error is 0.19 ± 0.17 .

The Monte Carlo simulation results are presented in Fig. 5. This result is similar to the experimental results in Fig. 4, with more photons reaching the detector at a thicker cartilage layer. The Monte Carlo simulation results support the assumption of an exponential relationship between cartilage thickness and the spectroscopic data.

Discussion

The main finding of this study is the possibility to extract objective information about cartilage thickness by studying the reflectance spectrum from the cartilage surface. The result implicates that it is possible to use a minimally invasive technique to characterise cartilage in connection with *in situ* diagnosis.

The reflectance spectrum from a condyle surface can be seen as a sum of spectra from cartilage and subchondral bone (containing blood). Typical spectra from cartilage and bone can be seen in Fig. 2. Cartilage contains relatively few cells which occupy 10-20% of its volume. The remainder is extracellular material which is highly hydrated and contains up to 80% water by weight. The material consists primarily of large hydrated proteoglycan aggregates, entrapped within a matrix of collagen fibrils. This fibre structure and the fact that absorption of water in the investigated wavelength region is low, gives reason to believe that the character of the cartilage spectrum is an effect of reduced scattering at longer wavelengths according to the Mie theory. Consequently, the cartilage layer acts as a diffuse reflector for photons, impeding them from reaching the highly absorbing subchondral bone.

We intended to assess cartilage thickness by studying the relative content of cartilage and bone components in the combined reflectance spectrum. By using this approach, the accuracy of cartilage thickness determination only becomes dependent upon the variability of the optical properties of these components. This variability remains to be investigated for a larger human material, after which it also will be possible to model the behavior for the complete spectrum and not just for a single wavelength. The exponential relationship between cartilage thickness and diffuse reflectance was expected (NÖTZLI et al., 1989).

A tentative source of error could be the variability of perfusion in the underlying bone. Flow rates in (rabbit) tibial and femoral cortical bone vary in a physiological range of 1.6 – 7.0 ml·min⁻¹·g⁻¹ (SHEPHERD and ÖBERG, 1990). Increased perfusion/blood content probably leads to increased absorption by the haemoglobin of the bone. Some of the data scattering in Fig. 4 may be due to the resolution of the ultrasound reference

system (0.06 mm according to the manufacturer's specifications). This value can be compared to the model mean error for thinner cartilage layers 0.19 ± 0.17 mm.

The accuracy of the ultrasound reference method depends on the ultrasound speed in cartilage (JURVELIN et al., 1995). Without a calibration of the device to cartilage ultrasound speed data we may have some spreading in data. Grinding causes roughening of the cartilage surface, affecting the degree of specular reflection. However, the specular reflection can be considered wavelength independent, not affecting the thickness estimation, solely based on specular distribution. For the same reason, the measurement distance was not precisely controlled.

To achieve maximal penetration depth, we chose to record the spectrum between 330 – 835 nm. It is reasonable to assume that a few characteristic wavelengths can be found that can be used for thickness calculations, thereby eliminating the need for recording the complete spectrum. Such an approach can facilitate the design of a future instrument based on the principle presented in the paper. An attractive feature of this principle is that it is based on fibre optics. Thus, it can probably be “imbedded” in an arthroscope, which, in addition to the visual assessment of the cartilage surface can give quantitative information about the thickness of the cartilage layer under study. Future challenges can involve the assessment of various aspects of cartilage quality such as the degree of fibrillation and surface roughness through fibre optic sensing.

We found a large variation in the thickness of the bovine hip joint cartilage (0.67 - 1.98 mm). The same variation can be found in human hip joint cartilage (1.14 - 2.84 mm), depending on where on the joint the cartilage is measured (NAKANISHI et al., 2001). There are reasons to believe that hip joints can be assessed through the sterile introduction of a fibre optic bundle but the most interesting application for this new principle may be the assessment of the knee via arthroscopy. The cartilage thickness of healthy and osteoarthritic human knee joints varies in the range of 0.5 to 7.4 mm (KLADNY et al., 1999). With the present method the haemoglobin absorption peaks could often be seen for thicker cartilage layers (Fig. 3) but a clear spectral effect occurred at cartilage thicknesses below 0.5 mm. In a well-perfused bone the variation and sensitivity of the method may be improved. Penetration depth may also be improved by focusing on the diffuse reflection component, by using more efficient optical components and by geometrical separation of light source and detector. Blood perfusion of bone has, for instance, been measured at 3.5 mm penetration depth, including

penetration of a 1 mm thick cartilage layer, using a 632.8 nm laser Doppler technique (NÖTZLI et al., 1999).

Conclusions

5

After studying bovine hip joint condyle surfaces, it was found that information about cartilage thickness could be extracted using optical reflectance spectroscopy. For thicker cartilage layers, a high reflection for the wavelengths 400-600 nm was seen, and for thinner cartilage layers, the characteristic spectra of blood and bone dominated.

10 Consequently, the optical reflectance spectrum may be used to characterise cartilage, and specifically cartilage thickness, in connection with *in situ* diagnosis.

References

- ARMSTRONG, C. G., and MOW, V. C. (1982): 'Variations in the intrinsic mechanical
15 properties of human articular cartilage with age, degeneration and water content', *Am. J. Bone Joint Surg.*, **64A**, pp. 88-94
- BEEK, J. F., BLOKLAND, P., POSTHUMUS, P., et al. (1997): 'In vitro double
integrating-sphere optical properties of tissues between 630 and 1064 nm', *Phys. Med. Biol.*, **42**, pp. 2255-2261
- 20 BRAUNSTEIN, E. M., BRANDT, K. D., and ALBRECHT, M. (1990): 'MRI demonstration of hypertrophic articular repair in osteoarthritis', *Skel. Radiol.*, **19**, pp. 335-339
- DE MUL, F. F. M., KOELINK, M. H., KOK, M. L., et al. (1995): 'Laser Doppler
velocimetry and Monte Carlo simulations on models for blood perfusion in tissue',
25 *Applied Optics*, **34**, pp. 6595-6611
- DREXLER, W., STAMPER, D., JESSER, C., et al. (2001): 'Correlation of collagen
organization with polarization sensitive imaging of in vivo cartilage: Implications for
osteoarthritis', *J. Rheumatol.*, **28**, pp. 1311-18.
- FIRBANK, M., HIRAOKA, M., ESSENPREIS, M., and DELPY, D. T. (1993):
30 'Measurement of the optical properties of the skull in the wavelength range 650-950
nm', *Phys. Med. Biol.*, **38**, pp. 503-510
- HALL, F. M., and WYSHAK, G. (1980): 'Thickness of cartilage in the normal knee', *J. Bone Joint. Surg.*, **62A**, pp. 408-413

- HANDLEY, R. C., ESSEX, T., and POOLEY, J. (1990): 'Laser Doppler flowmetry and bone blood flow in an isolated perfusion preparation', *J. Med. Eng. Technol.*, **14**, pp. 201-204
- 5 HERRMANN, J. M., PITRIS C., BOUMA, B. E., et al. (1999): 'High resolution imaging of normal and osteoarthritic cartilage with optical coherence tomography', *J. Rheumatol.*, **26**, pp. 627-635
- HOCH, D. H., GRODZINSKY, A. J., KOOB, T. J., et al. (1983): 'Early changes in material properties of rabbit articular cartilage after meniscectomy', *J. Orthop. Res.*, **1**, pp. 4-12
- 10 JACKSON, R. W. (1983): 'Current concepts review: Arthroscopic surgery', *J. Bone Joint Surg.*, **65**, pp. 416-420
- JURVELIN, J. S., RÄSÄNEN, T., KOLMONEN, P., and LYYRA, T. (1995): 'Comparison of optical needle probe and ultrasound technique for measurement of articular cartilage thickness', *J. Biomechanics*, **28**, pp. 231-235
- 15 KLDADNY, B., MARCUS, P., SCHIWY-BOCHAT, K.-H., et al. (1999): 'Measurement of cartilage thickness in the human knee-joint by magnetic resonance imaging using a three-dimensional gradient-echo sequence', *International Orthopaedics*, **23**, pp. 264-267
- LEHNER, K. B., RECHL, H. P., GMENWIESER, J. K., et al. (1989): 'Structure, function and degeneration of bovine hyaline cartilage: assessment with MR imaging *in-vitro*', *Radiology*, **170**, pp. 495-499
- 20 MAH, E. T., LANGLOIS, S. P., LOTT, C. W., LEE, W. K., BROWN, G. (1990): 'Detection of articular defects using magnetic resonance imaging: an experimental study', *Aust. N. Z. Surg.*, **60**, pp. 977-981
- MODEST, V. E., MURPHY, M. C., and MANN, R. W. (1989): 'Optical verification of a technique for in situ ultrasonic measurement of articular cartilage thickness', *J. Biomechanics*, **22**, pp. 171-176
- 25 MOW, V. C., GIBBS, M. C., LAI, W. M., ZHU, W. B., and ATHANASIOU, K. A. (1989): 'Biphasic indentation of articular cartilage. II - A numerical algorithm and an experimental study', *J. Biomechanics*, **22**, pp. 853-861
- 30 NAKANISHI, K., TANAKA, H., SUGANO, N., et al. (2001): 'MR-based three-dimensional presentation of cartilage thickness in the femoral head', *Eur. Radiol.*, **11**, pp. 2178-83

NÖTZLI, H. P., SWIONTKOWSKI, M. F., THAXTER, S. T., et al. (1989): 'Laser Doppler flowmetry for bone blood flow measurements: Helium-neon laser light attenuation and depth of perfusion assessment', *J. Orthopaedic Res.*, **7**, pp. 413-424

PEYRON, J. G. (1986): 'Osteoarthritis. The epidemiologic viewpoint', *Clin. Orthop.*, **213**, pp. 13-19

RECHT, M. P., and RESNICK, D. (1994): 'MR imaging of articular cartilage: current status and future directions', *AJR*, **163**, pp. 283-290

RUSHFELDT, P. D., MANN, R. W., and HARRIS, W. H. (1981): 'Improved techniques for measuring in vitro. The geometry and pressure distribution in the human acetabulum. I - Ultrasonic measurement of acetabular surfaces, sphericity and cartilage thickness', *J. Biomechanics*, **14**, pp. 252-260

RÄSÄNEN, T., JURVELIN, J., and HELMINEN, H. J. (1990): 'Indentation and shear tests of bovine knee articular cartilage', *Biomech. Sem.*, **5**, pp. 22-28

SHEPHERD, A. P., and ÖBERG, P. Å (eds) (1990): 'Laser-Doppler Flowmetry', Kluwer Academic Publishers

SWANN, A. C., and SEEDHOM, B. B. (1989): 'Improved technique for measuring the indentation and thickness of articular cartilage', *Proc. Inst. Mech. Eng.*, **203**, pp. 143-150

TAGAKI, K. (1918) quoted in ALTMAN, R. D., and KATES, J. (1983): 'Arthroscopy of the knee', *Semin. Arthritides. Rheum.*, **13**, pp. 188-199

TAKATANI, S., and GRAHAM, M. D. (1979): 'Theoretical analysis of diffuse reflectance from a two-layer tissue model', *IEEE Trans. Biomed. Eng.*, **BME-26**, pp. 656-664

TUCHIN, V. (2000): 'Tissue optics – Light scattering methods and instruments for medical diagnosis', *Tutorial texts in optical engineering*, Volume TT38, SPIE Press, Washington, USA

WAYNE, J. S., BRODRICK, C. W., and MUKHERIE, N. (1998): 'Measurement of articular cartilage thickness in the articulated knee', *Ann. Biomed. Engng.*, **26**, pp. 96-102

Technical solution 1

Single point measurement by white light illumination, spectroscopic detection and signal processing for calculating intensity ratios to determine cartilage thickness. Suitable ratios are $\lambda_1/\lambda_{\text{ref}}$ or $\lambda_2/\lambda_{\text{ref}}$, where λ_{ref} is a reference wavelength, possibly 630 nm, λ_1 is a haemoglobin absorption peak (425, 542 or 576 nm) and λ_2 is an infrared wavelength with high water absorption, possibly 1100 nm.

The solution is presented in Fig. 6 and Fig. 7. White light is supplied by a light source (15) emitting light into fiber bundle 1 (3). The light source is driven by a light source driver unit (14), stabilized by a control unit (13). The light source could be a broad band tungsten lamp. All fiber bundles could consist of high aperture optical glass fibers. Fiber bundle 1 (3) is passing through a channel (5) in the extension (9) of the arthroscopic probe (10) and supplies illumination of the measurement object (11) via a lens (6). This light serves both as illumination for investigation and for measurement. Light reflected from the object (11) is collected via the lens (6) into fiber bundle 2 (8). Fiber bundle 2 (8) passes through the same channel (5) and the intensity of light is measured by a detection unit (16) after manual input via an input device (12) requesting measurement to start. The detection unit is located in a control apparatus (19) and could be a CCD spectrometer. The detected signal is processed in a signal processor (17) according to the theory presented above. Cartilage thickness result is presented on a display unit (18). One solution of the arthroscopic probe (10) includes channels for saline perfusion and suction (4) and an ocular channel (1) for visual observation through an eyepiece (7) during the measurement. The visual image can be focused using a screw (2).

Technical solution 2

Single point measurement by discrete wavelength illumination, detection and signal processing for calculating intensity ratios to determine cartilage thickness. Chosen wavelengths could be λ_1 , λ_2 and λ_{ref} , giving ratios $\lambda_1/\lambda_{\text{ref}}$ and $\lambda_2/\lambda_{\text{ref}}$, where λ_{ref} is a reference wavelength, possibly 630 nm, λ_1 is a haemoglobin absorption peak (425, 542 or 576 nm) and λ_2 is an infrared wavelength with high water absorption, possibly 1100 nm.

The solution is presented in Fig. 6 and Fig. 7. Both white light and discrete wavelength light are supplied by light sources (15) emitting light into fiber bundle 1 (3). The light sources are driven by a light source driver unit (14), stabilized by a control unit (13).

The light sources could be a broad band tungsten lamp and stable light emitting diodes.

- 5 All fiber bundles could consist of high aperture optical glass fibers. Fiber bundle 1 (3) is passing through a channel (5) in the extension (9) of the arthroscopic probe (10) and supplies illumination of the measurement object (11) via a lens (6). The white light serves as illumination for investigation and the discrete wavelength light for measurement. Light reflected from the object (11) is collected via the lens (6) into fiber bundle 2
- 10 (8). Fiber bundle 2 (8) passes through the same channel (5) and the intensity of light is measured by a detection unit (16) after manual input via an input device (12) requesting measurement to start. At measurement start, the white light source is turned off, as controlled by the control unit (13). The detection unit (16) is located in a control apparatus (19) and could consist of photo diodes. The detected signal is processed in a signal
- 15 processor (17) according to the theory presented above. Cartilage thickness result is presented on a display unit (18). One solution of the arthroscopic probe (10) includes channels for saline perfusion and suction (4) and an ocular channel (1) for visual observation through an eyepiece (7) during the measurement. The visual image can be focused using a screw (2).

20

Technical solution 3

Imaging by using white light illumination, optical filters and/or signal processing for creating images with enhanced contrast between cartilage and bone, and/or contrast

between fibrillated and healthy cartilage. Chosen wavelengths could be λ_1 , λ_2 and λ_{ref}

- 25 giving ratios $\lambda_1/\lambda_{\text{ref}}$ or $\lambda_2/\lambda_{\text{ref}}$, where λ_{ref} is a reference wavelength, possibly 630 nm, λ_1 is a haemoglobin absorption peak (425, 542 or 576 nm) and λ_2 is an infrared wavelength with high water absorption, possibly 1100 nm.

The solution is presented in Fig. 6 and Fig. 7. White light is supplied by a light source (15) emitting light into fiber bundle 1 (3). The light source is driven by a light source

30

driver unit (14), stabilized by a control unit (13). The light source could be a broad band tungsten lamp. The fiber bundles could consist of high aperture optical glass fibers.

Fiber bundle 1 (3) is passing through a channel (5) in the extension (9) of the

arthroscopic probe (10) and supplies illumination of the measurement object (11) via a lens (6). This light serves both as illumination for investigation and measurement. Light reflected from the object (11) is collected via the lens (6) into fiber bundle 2 (8). In one solution polarization filters are included at the fiber tip for the measurement of cartilage fibrillation. Fiber bundle 2 (8) passes through the same channel (5) and the intensity of light is measured by a detection unit (16) after manual input via an input device (12) requesting measurement to start. The detection unit (16) is located in a control apparatus (19) and could consist of a 2D CCD array. In one solution, the detection device includes optical filters before detection, and in another solution, image processing is performed digitally after detection by a signal processor (17), in both cases according to the theory presented above. Contrast enhanced images of the measurement object (11) is presented on a display unit (18). One solution of the arthroscopic probe (10) includes channels for saline perfusion and suction (4) and an ocular channel (1) for visual observation through an eyepiece (7) during the measurement. The visual image can be focused using a screw (2).

CLAIMS

1. Device for measuring joint cartilage qualities, such as cartilage thickness, cartilage surface roughness and degree of cartilage fibrillation, comprising an arthroscopic probe
5 (19) with an extension (9) for inspection of the joint, wherein fiber bundles (3, 8) are arranged in said extension c h a r a c t e r i z e d i n

that the fibre bundles include a first set of fibers (3) for conveying light from a light source (15) to illuminate the joint surface and a second set of fibers (8) for conveying light reflected from the joint surface to a detector means
10 (16),

that said detector means (16) is designed for measuring the intensity of light reflected from the joint surface.

2. Device in accordance with claim 1, wherein said detector means (16) is a light
15 intensity detector for single wavelengths or for a spectrum of wavelengths, that is connected to a signal processor (17), provided in a control apparatus (19), said signal processor being configured to apply a cartilage thickness algorithm on data acquired from said detector means (16).

20 3. Device in accordance with claim 2, wherein said cartilage thickness algorithm utilizes the fact that the photon absorption of cartilage and subchondral bone is different at wavelength regions related to blood chromophores or water.

4. Device in accordance with claim 1, wherein said detector means (16) is a light
25 intensity detector for single wavelengths or for a spectrum of wavelengths, sensitive to polarization state of measured light, that is connected to a signal processor (17), provided in a control apparatus (19), said signal processor being configured to apply a cartilage fibrillation algorithm on data acquired from said detector means (16).

30 5. Device in accordance with claim 4, wherein said cartilage fibrillation algorithm utilizes the fact that the polarization states of photons are different after back-scattering by healthy or diseased/arthritic cartilage.

6. Device for imaging joint surfaces, enhancing contrast between healthy and diseased/arthritic regions, including thin cartilage regions, regions with rough surface cartilage and regions with highly fibrillated cartilage, comprising an arthroscopic probe (19) with an extension (9) for inspection of the joint, wherein fiber bundles (3, 8) are

5 arranged in said extension characterized in

that the fibre bundles include a first set of fibers (3) for conveying light from a light source (15) to illuminate the joint surface and a second set of fibers (8) for conveying light reflected from the joint surface to an two-dimensional detector means (16),

10 that said two-dimensional detector means (16) is designed to present the intensity of light reflected from the joint surface.

7. Device in accordance with claim 6, wherein said two-dimensional detector means (16) is a light intensity detector for single wavelengths or for a spectrum of wavelengths,

15 that is connected to a signal processor (17), provided in a control apparatus (19), said signal processor being configured to apply a cartilage thickness algorithm on data acquired from said two-dimensional detector means (16).

8. Device in accordance with claim 7, wherein said cartilage thickness algorithm utilizes the fact that the photon absorption of cartilage and subchondral bone is different at wavelength regions related to blood chromophores or water.

9. Device in accordance with claim 6, wherein said two-dimensional detector means (16) is a light intensity detector for single wavelengths or for a spectrum of wavelengths,

25 sensitive to polarization state of measured light, that is connected to a signal processor (17), provided in a control apparatus (19), said signal processor being configured to apply a cartilage fibrillation algorithm on data acquired from said two-dimensional detector means (16).

30 10. Device in accordance with claim 9, wherein said cartilage fibrillation algorithm utilizes the fact that the polarization states of photons are different after back-scattering by healthy or diseased/arthritic cartilage.

11. Method for measuring joint cartilage qualities, such as cartilage thickness, cartilage surface roughness and degree of cartilage fibrillation, according to claims 1-10.

5

ABSTRACT

The invention described is an arrangement and a method for measuring joint cartilage qualities, such as cartilage thickness, cartilage surface roughness and degree of cartilage fibrillation. The arrangement comprises an arthroscopic probe (19), fiber bundles (3, 8), a light source (15) for emitting light, a detection unit (16) for detecting reflected light, and a signal processor (17) for processing the detected signals. The arrangement utilizes a new principle for cartilage layer thickness assessment in joints, based on the differences in absorption spectrum between cartilage and subchondral bone, and a new principle for cartilage fibrillation assessment, based on the differences in photon polarization state between light back-scattered from healthy or diseased/arthritic cartilage.

2
3
4
5
6
7
8
9
10
11
12
13
14
15
16
17
18
19
20
21
22
23
24
25
26
27
28
29
30
31
32
33
34
35
36
37
38
39
40
41
42
43
44
45
46
47
48
49
50
51
52
53
54
55
56
57
58
59
60
61
62
63
64
65
66
67
68
69
70
71
72
73
74
75
76
77
78
79
80
81
82
83
84
85
86
87
88
89
90
91
92
93
94
95
96
97
98
99
100
101
102
103
104
105
106
107
108
109
110
111
112
113
114
115
116
117
118
119
120
121
122
123
124
125
126
127
128
129
130
131
132
133
134
135
136
137
138
139
140
141
142
143
144
145
146
147
148
149
150
151
152
153
154
155
156
157
158
159
160
161
162
163
164
165
166
167
168
169
170
171
172
173
174
175
176
177
178
179
180
181
182
183
184
185
186
187
188
189
190
191
192
193
194
195
196
197
198
199
200
201
202
203
204
205
206
207
208
209
210
211
212
213
214
215
216
217
218
219
220
221
222
223
224
225
226
227
228
229
230
231
232
233
234
235
236
237
238
239
240
241
242
243
244
245
246
247
248
249
250
251
252
253
254
255
256
257
258
259
260
261
262
263
264
265
266
267
268
269
270
271
272
273
274
275
276
277
278
279
280
281
282
283
284
285
286
287
288
289
290
291
292
293
294
295
296
297
298
299
300
301
302
303
304
305
306
307
308
309
310
311
312
313
314
315
316
317
318
319
320
321
322
323
324
325
326
327
328
329
330
331
332
333
334
335
336
337
338
339
340
341
342
343
344
345
346
347
348
349
350
351
352
353
354
355
356
357
358
359
360
361
362
363
364
365
366
367
368
369
370
371
372
373
374
375
376
377
378
379
380
381
382
383
384
385
386
387
388
389
390
391
392
393
394
395
396
397
398
399
400
401
402
403
404
405
406
407
408
409
410
411
412
413
414
415
416
417
418
419
420
421
422
423
424
425
426
427
428
429
430
431
432
433
434
435
436
437
438
439
440
441
442
443
444
445
446
447
448
449
450
451
452
453
454
455
456
457
458
459
460
461
462
463
464
465
466
467
468
469
470
471
472
473
474
475
476
477
478
479
480
481
482
483
484
485
486
487
488
489
490
491
492
493
494
495
496
497
498
499
500
501
502
503
504
505
506
507
508
509
510
511
512
513
514
515
516
517
518
519
520
521
522
523
524
525
526
527
528
529
530
531
532
533
534
535
536
537
538
539
540
541
542
543
544
545
546
547
548
549
550
551
552
553
554
555
556
557
558
559
560
561
562
563
564
565
566
567
568
569
570
571
572
573
574
575
576
577
578
579
580
581
582
583
584
585
586
587
588
589
590
591
592
593
594
595
596
597
598
599
600
601
602
603
604
605
606
607
608
609
610
611
612
613
614
615
616
617
618
619
620
621
622
623
624
625
626
627
628
629
630
631
632
633
634
635
636
637
638
639
640
641
642
643
644
645
646
647
648
649
650
651
652
653
654
655
656
657
658
659
660
661
662
663
664
665
666
667
668
669
670
671
672
673
674
675
676
677
678
679
680
681
682
683
684
685
686
687
688
689
690
691
692
693
694
695
696
697
698
699
700
701
702
703
704
705
706
707
708
709
710
711
712
713
714
715
716
717
718
719
720
721
722
723
724
725
726
727
728
729
730
731
732
733
734
735
736
737
738
739
740
741
742
743
744
745
746
747
748
749
750
751
752
753
754
755
756
757
758
759
760
761
762
763
764
765
766
767
768
769
770
771
772
773
774
775
776
777
778
779
780
781
782
783
784
785
786
787
788
789
790
791
792
793
794
795
796
797
798
799
800
801
802
803
804
805
806
807
808
809
810
811
812
813
814
815
816
817
818
819
820
821
822
823
824
825
826
827
828
829
830
831
832
833
834
835
836
837
838
839
840
841
842
843
844
845
846
847
848
849
850
851
852
853
854
855
856
857
858
859
860
861
862
863
864
865
866
867
868
869
870
871
872
873
874
875
876
877
878
879
880
881
882
883
884
885
886
887
888
889
890
891
892
893
894
895
896
897
898
899
900
901
902
903
904
905
906
907
908
909
910
911
912
913
914
915
916
917
918
919
920
921
922
923
924
925
926
927
928
929
930
931
932
933
934
935
936
937
938
939
940
941
942
943
944
945
946
947
948
949
950
951
952
953
954
955
956
957
958
959
960
961
962
963
964
965
966
967
968
969
970
971
972
973
974
975
976
977
978
979
980
981
982
983
984
985
986
987
988
989
990
991
992
993
994
995
996
997
998
999
1000
1001
1002
1003
1004
1005
1006
1007
1008
1009
1010
1011
1012
1013
1014
1015
1016
1017
1018
1019
1020
1021
1022
1023
1024
1025
1026
1027
1028
1029
1030
1031
1032
1033
1034
1035
1036
1037
1038
1039
1040
1041
1042
1043
1044
1045
1046
1047
1048
1049
1050
1051
1052
1053
1054
1055
1056
1057
1058
1059
1060
1061
1062
1063
1064
1065
1066
1067
1068
1069
1070
1071
1072
1073
1074
1075
1076
1077
1078
1079
1080
1081
1082
1083
1084
1085
1086
1087
1088
1089
1090
1091
1092
1093
1094
1095
1096
1097
1098
1099
1100
1101
1102
1103
1104
1105
1106
1107
1108
1109
1110
1111
1112
1113
1114
1115
1116
1117
1118
1119
1120
1121
1122
1123
1124
1125
1126
1127
1128
1129
1130
1131
1132
1133
1134
1135
1136
1137
1138
1139
1140
1141
1142
1143
1144
1145
1146
1147
1148
1149
1150
1151
1152
1153
1154
1155
1156
1157
1158
1159
1160
1161
1162
1163
1164
1165
1166
1167
1168
1169
1170
1171
1172
1173
1174
1175
1176
1177
1178
1179
1180
1181
1182
1183
1184
1185
1186
1187
1188
1189
1190
1191
1192
1193
1194
1195
1196
1197
1198
1199
1200
1201
1202
1203
1204
1205
1206
1207
1208
1209
1210
1211
1212
1213
1214
1215
1216
1217
1218
1219
1220
1221
1222
1223
1224
1225
1226
1227
1228
1229
1230
1231
1232
1233
1234
1235
1236
1237
1238
1239
1240
1241
1242
1243
1244
1245
1246
1247
1248
1249
1250
1251
1252
1253
1254
1255
1256
1257
1258
1259
1260
1261
1262
1263
1264
1265
1266
1267
1268
1269
1270
1271
1272
1273
1274
1275
1276
1277
1278
1279
1280
1281
1282
1283
1284
1285
1286
1287
1288
1289
1290
1291
1292
1293
1294
1295
1296
1297
1298
1299
1300
1301
1302
1303
1304
1305
1306
1307
1308
1309
1310
1311
1312
1313
1314
1315
1316
1317
1318
1319
1320
1321
1322
1323
1324
1325
1326
1327
1328
1329
1330
1331
1332
1333
1334
1335
1336
1337
1338
1339
1340
1341
1342
1343
1344
1345
1346
1347
1348
1349
1350
1351
1352
1353
1354
1355
1356
1357
1358
1359
1360
1361
1362
1363
1364
1365
1366
1367
1368
1369
1370
1371
1372
1373
1374
1375
1376
1377
1378
1379
1380
1381
1382
1383
1384
1385
1386
1387
1388
1389
1390
1391
1392
1393
1394
1395
1396
1397
1398
1399
1400
1401
1402
1403
1404
1405
1406
1407
1408
1409
1410
1411
1412
1413
1414
1415
1416
1417
1418
1419
1420
1421
1422
1423
1424
1425
1426
1427
1428
1429
1430
1431
1432
1433
1434
1435
1436
1437
1438
1439
1440
1441
1442
1443
1444
1445
1446
1447
1448
1449
1450
1451
1452
1453
1454
1455
1456
1457
1458
1459
1460
1461
1462
1463
1464
1465
1466
1467
1468
1469
1470
1471
1472
1473
1474
1475
1476
1477
1478
1479
1480
1481
1482
1483
1484
1485
1486
1487
1488
1489
1490
1491
1492
1493
1494
1495
1496
1497
1498
1499
1500
1501
1502
1503
1504
1505
1506
1507
1508
1509
1510
1511
1512
1513
1514
1515
1516
1517
1518
1519
1520
1521
1522
1523
1524
1525
1526
1527
1528
1529
1530
1531
1532
1533
1534
1535
1536
1537
1538
1539
1540
1541
1542
1543
1544
1545
1546
1547
1548
1549
1550
1551
1552
1553
1554
1555
1556
1557
1558
1559
1560
1561
1562
1563
1564
1565
1566
1567
1568
1569
1570
1571
1572
1573
1574
1575
1576
1577
1578
1579
1580
1581
1582
1583
1584
1585
1586
1587
1588
1589
1590
1591
1592
1593
1594
1595
1596
1597
1598
1599
1600
1601
1602
1603
1604
1605
1606
1607
1608
1609
1610
1611
1612
1613
1614
1615
1616
1617
1618
1619
1620
1621
1622
1623
1624
1625
1626
1627
1628
1629
1630
1631
1632
1633
1634
1635
1636
1637
1638
1639
1640
1641
1642
1643
1644
1645
1646
1647
1648
1649
1650
1651
1652
1653
1654
1655
1656
1657
1658
1659
1660
1661
1662
1663
1664
1665
1666
1667
1668
1669
1670
1671
1672
1673
1674
1675
1676
1677
1678
1679
1680
1681
1682
1683
1684
1685
1686
1687
1688
1689
1690
1691
1692
1693
1694
1695
1696
1697
1698
1699
1700
1701
1702
1703
1704
1705
1706
1707
1708
1709
1710
1711
1712
1713
1714
1715
1716
1717
1718
1719
1720
1721
1722
1723
1724
1725
1726
1727
1728
1729
1730
1731
1732
1733
1734
1735
1736
1737
1738
1739
1740
1741
1742
1743
1744
1745
1746
1747
1748
1749
1750
1751
1752
1753
1754
1755
1756
1757
1758
1759
1760
1761
1762
1763
1764
1765
1766
1767
1768
1769
1770
1771
1772
1773
1774
1775
1776
1777
1778
1779
1780
1781
1782
1783
1784
1785
1786
1787
1788
1789
1790
1791
1792
1793
1794
1795
1796
1797
1798
1799
1800
1801
1802
1803
1804
1805
1806
1807
1808
1809
1810
1811
1812
1813
1814
1815
1816
1817
1818
1819
1820
1821
1822
1823
1824
1825
1826
1827
1828
1829
1830
1831
1832
1833
1834
1835
1836
1837
1838
1839
1840
1841
1842
1843
1844
1845
1846
1847
1848
1849
1850
1851
1852
1853
1854
1855
1856
1857
1858
1859
1860
1861
1862
1863
1864
1865
1866
1867
1868
1869
1870
1871
1872
1873
1874
1875
1876
1877
1878
1879
1880
1881
1882
1883
1884
1885
1886
1887
1888
1889
1890
1891
1892
1893
1894
1895
1896
1897
1898
1899
1900
1901
1902
1903
1904
1905
1906
1907
1908
1909
1910
1911
1912
1913
1914
1915
1916
1917
1918
1919
1920
1921
1922
1923
1924
1925
1926
1927
1928
1929
1930
1931
1932
1933
1934
1935
1936
1937
1938
1939
1940
1941
1942
1943
1944
1945
1946
1947
1948
1949
1950
1951
1952
1953
1954
1955
1956
1957
1958
1959
1960
1961
1962
1963
1964
1965
1966
1967
1968
1969
1970
1971
1972
1973
1974
1975
1976
1977
1978
1979
1980
1981
1982
1983
1984
1985
1986
1987
1988
1989
1990
1991
1992
1993
1994
1995
1996
1997
1998
1999
2000
2001
2002
2003
2004
2005
2006
2007
2008
2009
2010
2011
2012
2013
2014
2015
2016
2017
2018
2019
2020
2021
2022
2023
2024
2025
2026
2027
2028
2029
2030
2031
2032
2033
2034
2035
2036
2037
2038
2039
2040
2041
2042
2043
2044
2045
2046
2047
2048
2049
2050
2051
2052
2053
2054
2055
2056
2057
2058
2059
2060
2061
2062
2063
2064
2065
2066
2067
2068
2069
2070
2071
2072
2073
2074
2075
2076
2077
2078
2079
2080
2081
2082
2083
2084
2085
2086
2087
2088
2089
2090
2091
2092
2093
2094
2095
2096
2097
2098
2099
2100
2101
2102
2103
2104
2105
2106
2107
2108
2109
2110
2111
2112
2113
2114
2115
2116
2117
2118
2119
2120
2121
2122
2123
2124
2125
2126
2127
2128
2129
2130
2131
2132
2133
2134
2135
2136
2137
2138
2139
2140
2141
2142
2143
2144
2145
2146
2147
2148
2149
2150
2151
2152
2153
2154
2155
2156
2157
2158
2159
2160
2161
2162
2163
2164
2165
2166
2167
2168
2169
2170
2171
2172
2173
2174
2175
2176
2177
2

Figure 1

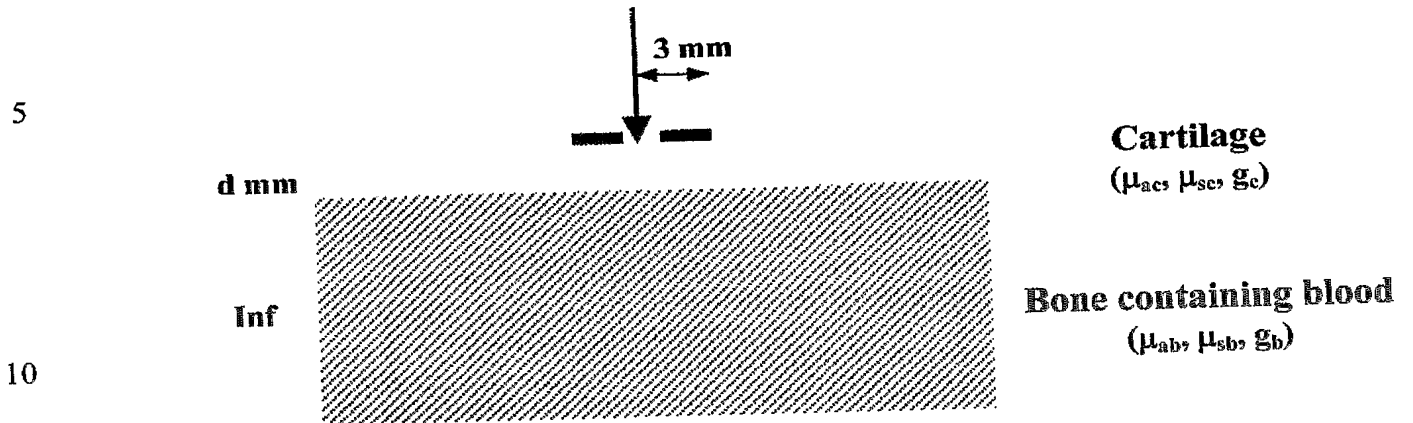


Figure 2

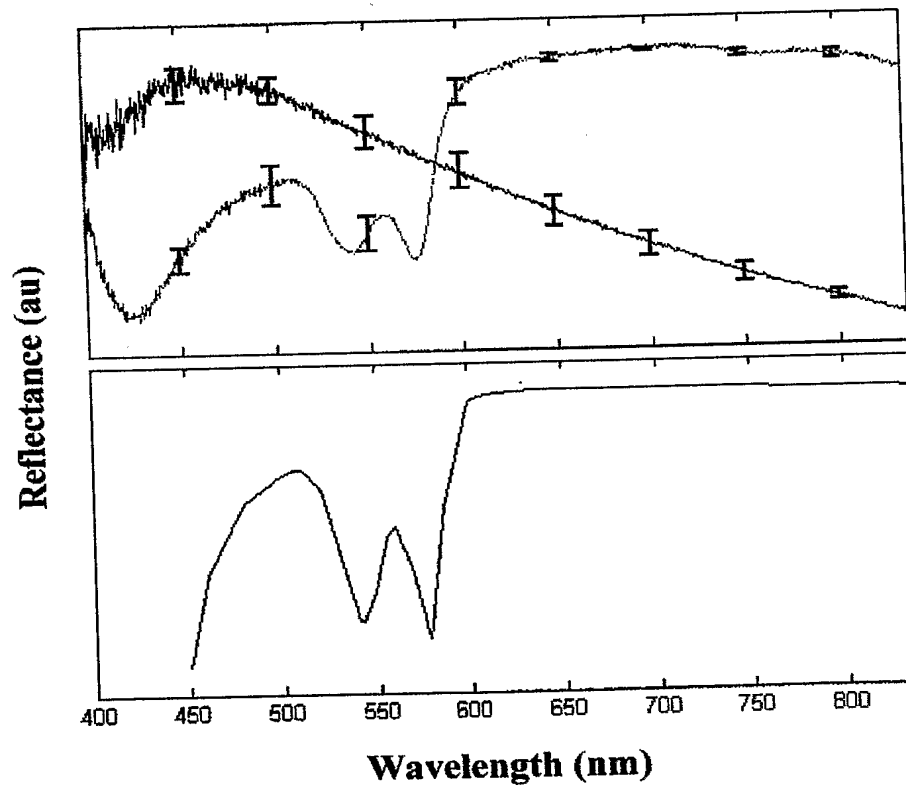
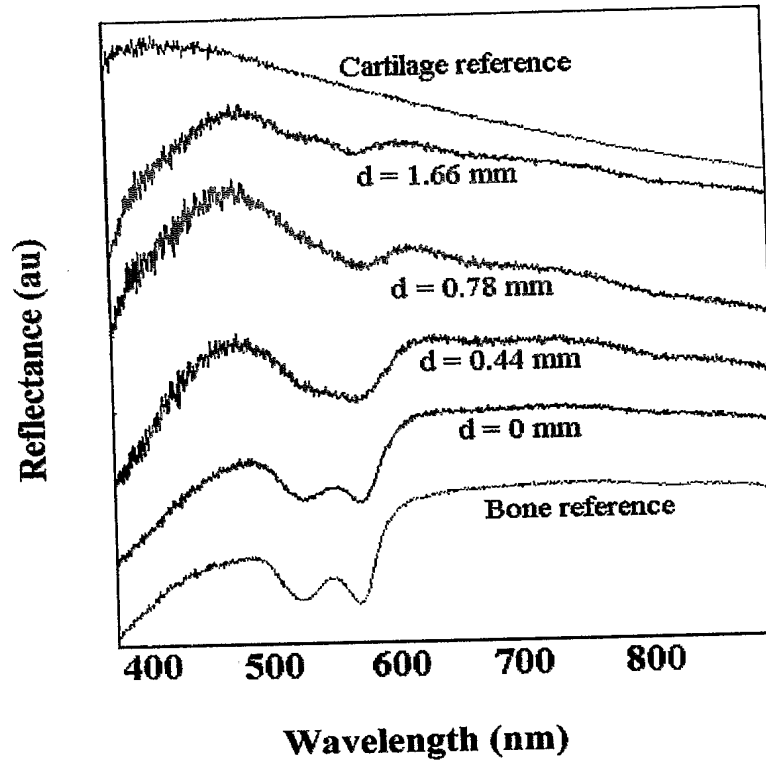
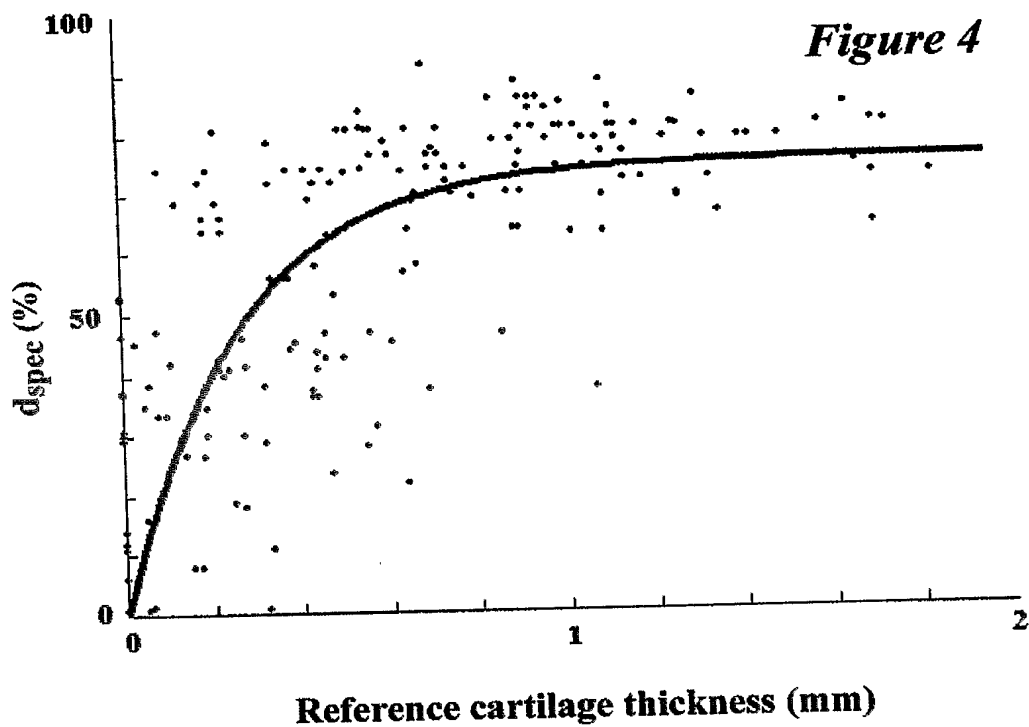
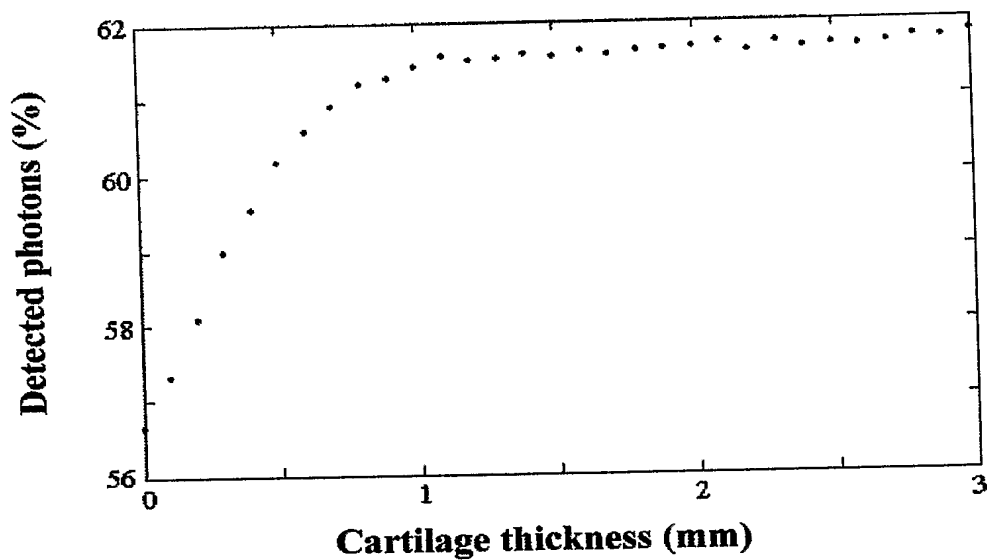


Figure 3





5

Figure 5

23

Figure 6

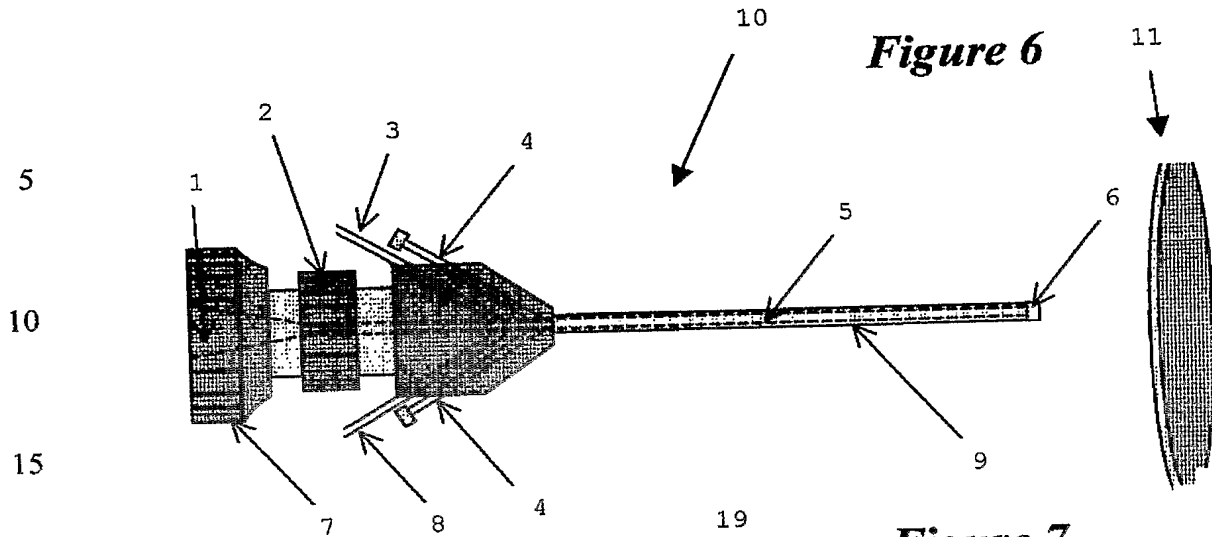
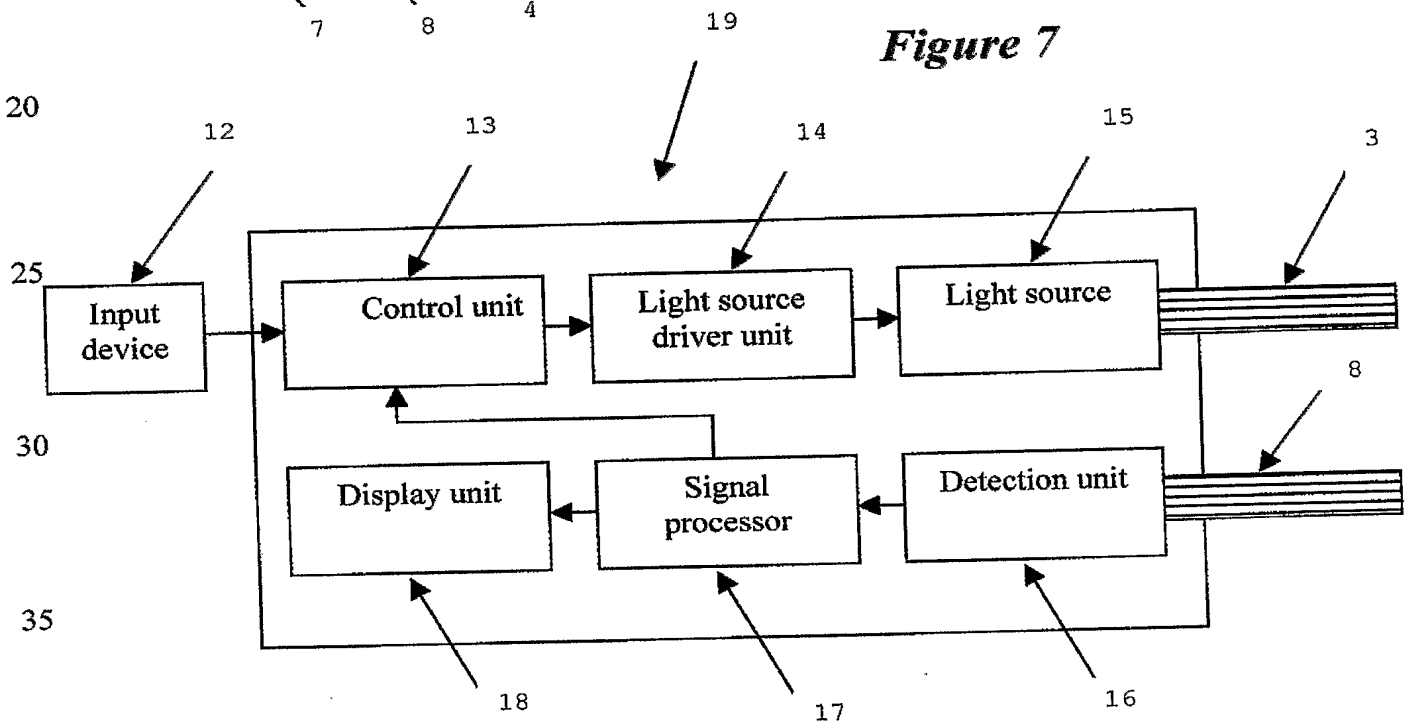


Figure 7



1	Ocular channel	11	Measurement object
2	Focusing screw	12	Input device
3	Fiber bundle 1	13	Control unit
4	Channels for saline perfusion/suction	14	Light source driver unit
5	Channels through extension	15	Light source
6	Lens	16	Detection unit
7	Eyepiece	17	Signal processor
8	Fiber bundle 2	18	Display unit
9	Extension	19	Control apparatus
10	Arthroscopic probe		